

In-silico identification of pyrazole derivatives as selective PDE7 inhibitors: ADME, docking, and toxicity profiling

Rishab Bhanot¹, Ajmer Singh Grewal² and Anjana Devi^{1*}

¹Department of Pharmacy, School of Pharmaceutical and Health Sciences, Career Point University, Hamirpur, Himachal Pradesh, 176041.

²Guru Gobind Singh College of Pharmacy, Yamuna Nagar, Haryana, India, 135001.

*Corresponding Author
Anjana Devi
(anjana.pharmacy@cpuh.edu.in)

Article History

Received: 21/09/2025

Revised: 30/09/2025

Accepted: 27/10/2025

Published: 24/11/2025

Abstract: The pathological process of inflammation is a major pathophysiology in the background of many chronic illnesses. Phosphodiesterase 7 (PDE7) is an immune system control enzyme, targeting which is a promising method of treating diseases. This paper involved the development and evaluation of new pyrazole analogues that could be used as PDE7 inhibitors by in-silico techniques, such as ADME prediction, molecular docking, and toxicity. The compounds that were designed had good oral bioavailability and drug-likeness that met the rule of five by Lipinski. Molecular docking experiments which were further supported by the re-docking of co-crystallised PDE7 ligand showed that some of the compounds, especially compounds 6, 12, 20 and 21, formed strong binding affinities and had long-term interactions with key active site residues of PDE7. Predictive toxicity tool, pkCSM revealed that certain compounds could produce mutations and liver damage, and skin irritation, whereas others have good toxicity. Overall, these findings suggest that pyrazole-like scaffolds may be promising as the subject of the creation of selective PDE7 inhibitors yet further experimentation in the laboratory and in living organisms is required.

Keywords: PDE7 inhibitors, Pyrazole derivatives, Drug-likeness, Molecular docking, Toxicity prediction, Inflammation.

INTRODUCTION

Inflammation is a complicated biological reaction and is injurious if the stimulus is a pathogen, damaged cells, or irritants [1]. It helps remove the cause, clear away dead cells, and start the healing process. Acute inflammation develops rapidly and is always associated with redness, heat, swelling, pain, and loss of function [2]. Chronic inflammation on the other end, develops over longer periods and is frequently encountered in autoimmune diseases, cancer, neurodegeneration, and metabolic disorders. Some of the immune cells during inflammation that are actively involved include macrophages and neutrophils; chemical mediators include cytokines, histamines, and prostaglandins; vascular changes include vasodilation and permeability [3]. So, while inflammation is generally a good thing for protection and healing, uncontrolled or excessive inflammation leads to damage. Anti-inflammatory medications and immunomodulators are then utilized to regulate inflammation in some of these conditions [4-15]. The limits of an anti-inflammatory approach are that cytokine inhibitors, through those effects, can also suppress immunity and perhaps increase susceptibility to infection, NSAIDs or COX inhibitors could cause gastric ulcers, renal dysfunction, or cardiovascular problems [16,17]. Targeting pathways such as NF- κ B or JAK-STAT may change normal cell functions leading to unwanted effects. Antioxidants mostly showed limited success, while pro-resolving mediators are still to be thoroughly researched and rather vague about the long-term effects [18]. Thus, despite advancements, precise targeting coupled with minimal off-target effects continues to be a daunting challenge in anti-

inflammatory therapy. As the existing ones have some limitations immunosuppression, side-effects, high cost, and non-specific targets-exploration is shifting toward newer targets such as phosphodiesterase 7 (PDE7) [19,20]. PDE7 regulates intracellular cAMP, which is a key player in the control of immune activation of cells [21]. The inhibition of PDE7 will modulate inflammation and leave the immune system relatively intact. This might avoid side effects, thus making PDE7 inhibitors a safer and more targeted approach in the treatment of chronic inflammatory disorders, especially when current interventions are either not fully helpful or are too risky [22,23]. Thus, this positions PDE7 as a therapeutic target worthy of being pursued in future drug design for anti-inflammation. Pyrazole is a five-membered heterocycle known to contain nitrogen. It has been studied intensively with respect to anti-inflammatory activity [24-28]. Pyrazole derivatives inhibit the important enzymes COX and LOX involved in corticosteroid biosynthesis, with subsequent reduction in production of numerous pro-inflammatory mediators, e.g., prostaglandins and leukotrienes [29-33]. Other studies have also shown that a few of these pyrazole compounds modulate cytokine production with effectiveness in several inflammation models (*in-vitro* and *in-vivo*) [34-36]. Celecoxib, a pyrazole derivative, acts as a selective COX-2 inhibitor for therapeutic uses [37]. Therefore, the present study aimed to design novel pyrazole derivatives and evaluate their potential as PDE7 inhibitors using *in-silico* approaches, including molecular docking, ADME profiling, and toxicity prediction, to identify promising candidates for the development of safer and more effective anti-inflammatory agents.

MATERIALS AND METHODS:

Prediction of Drug-Like Properties:

In-silico approaches for the determination of absorption, distribution, metabolism, and excretion (ADME) parameters rely on theoretically formulated statistical models. In the present study, all the designed compounds (Table 1) were evaluated for their ADME properties using SwissADME (<http://www.swissadme.ch/>), which provides a comprehensive platform for the estimation of pharmacokinetic profiles, physicochemical descriptors, and drug-likeness of small molecules. Also, the compounds' drug-likeness was measured using Lipinski's Rule of Five, a well-known rule that looks at the essential molecular characteristics of a molecule to evaluate their oral bioavailability [38-40].

Molecular Docking:

AutoDock Vina and AutoDock Tools had been used to perform *in-silico* docking investigations of the designed molecules [41-42]. The Protein Data Bank provided the PDE7 enzyme's crystal structure (PDB ID: 4PM0). Using AutoDock Tools, the protein structure was created by eliminating water molecules and existing ligands and adding the missing hydrogen atoms. The resulting protein structure was saved in docking-ready PDBQT

format after non-polar hydrogens were combined and polar hydrogens were added. Using MarvinSketch (ChemAxon), the two-dimensional chemical structures of every ligand, both standard and invented compounds, were created and then transformed into three-dimensional conformations (mol2 format). AutoDock Tools was used to further process Ligand files and save them in PDBQT format. The grid box dimensions were $40 \times 40 \times 40$, and the docking grid center was set at $X = -45.645$, $Y = 25.947$, and $Z = 1.043$. The co-crystallized ligand (from PDB ID: 4PM0) was re-docked into the PDE7 structure and its binding to a reference PDE7 inhibitor was compared to verify the docking procedure. The 3D-optimized ligands were then docked into the improved protein structure, and the log files were used to record their binding free energies (ΔG , kcal/mol). PyMOL (Schrödinger, LLC) and BIOVIA Discovery Studio Visualizer (Dassault Systemes) were used to investigate the binding interactions of the ligands in the PDE7 active site [43].

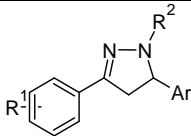
Prediction of Toxicity:

All the designed compounds were evaluated *in-silico* for potential toxicity predictions using the "pkCSM" web-based tool [44-45].

RESULTS & DISCUSSION:

Prediction of Drug-Likeness:

In-silico techniques play a vital role in the preliminary stages of drug discovery, particularly in predicting the pharmacokinetic behavior of compounds, commonly referred to as ADME [38]. SwissADME computes critical parameters including gastrointestinal (GI) absorption, blood-brain barrier (BBB) permeability, P-glycoprotein (P-gp) substrate identification, cytochrome P450 (CYP450) enzyme inhibition, and skin permeability (Log Kp), among others. According to Lipinski's rule, a compound is more likely to exhibit good oral bioavailability if it meets the following criteria: molecular weight (Mol. Wt.) ≤ 500 Da; LogP (octanol-water partition coefficient) ≤ 5 ; number of hydrogen bond donors (HBDs) ≤ 5 ; number of hydrogen bond acceptors (HBAs) ≤ 10 . Compounds that conform to these rules are typically regarded as having favorable pharmacokinetic characteristics and are more likely to succeed as orally active drug candidates [39,46]. The results obtained from the ADME study revealed that the designed compounds exhibited good pharmacokinetic parameters for oral bioavailability (Table 1) and conformed to Lipinski's rule of five for drug-likeness.

												
Sr. No.	R ¹	R ²	Ar	Mol. Wt.	Log P	HBAs	HBDs	NRBs	TPSA	GI ab.	BBB permeant	Lipinski
1	H	H	C ₆ H ₅	222.29	2.91	1	1	2	24.39	High	Yes	Yes
2	H	H	4-CH ₃ OC ₆ H ₄	252.31	2.88	2	1	3	33.62	High	Yes	Yes
3	H	H	4-Cl-C ₆ H ₄	222.29	2.91	1	1	2	24.39	High	Yes	Yes
4	3-NO ₂	H	C ₆ H ₅	285.30	2.01	4	2	3	74.05	High	Yes	Yes
5	3-NO ₂	H	4-CH ₃ OC ₆ H ₄	297.31	2.12	4	1	4	83.28	High	No	Yes

6	3-NO ₂	H	4-Cl-C ₆ H ₄	285.30	2.01	4	2	3	70.21	High	Yes	Yes
7	4-CH ₃	H	C ₆ H ₅	236.31	3.24	1	1	2	24.39	High	Yes	Yes
8	4-CH ₃	H	4-CH ₃ OC ₆ H ₄	266.34	3.22	2	1	3	33.62	High	Yes	Yes
9	4-CH ₃	H	4-Cl-C ₆ H ₄	270.76	3.78	1	1	2	24.39	High	Yes	Yes
10	4-OCH ₃	H	C ₆ H ₅	252.31	2.90	2	1	3	33.62	High	Yes	Yes
11	4-OCH ₃	H	4-CH ₃ OC ₆ H ₄	282.34	2.87	3	1	4	42.85	High	Yes	Yes
12	4-OCH ₃	H	4-Cl-C ₆ H ₄	286.76	3.42	2	1	3	33.62	High	Yes	Yes
13	4-Br	H	C ₆ H ₅	301.18	3.53	2	1	2	24.39	High	Yes	Yes
14	4-Br	H	4-CH ₃ OC ₆ H ₄	331.21	3.51	2	1	3	33.62	High	Yes	Yes
15	4-Br	H	4-Cl-C ₆ H ₄	335.63	4.06	1	1	2	24.39	High	Yes	Yes
16	H	CH ₃	C ₆ H ₅	236.31	3.11	1	0	2	15.60	High	Yes	Yes
17	H	CH ₃	4-CH ₃ OC ₆ H ₄	266.34	3.07	2	0	3	24.83	High	Yes	Yes
18	H	CH ₃	4-Cl-C ₆ H ₄	270.76	3.65	1	0	2	15.60	High	Yes	Yes
19	3-NO ₂	CH ₃	C ₆ H ₅	281.31	2.30	3	0	3	61.42	High	Yes	Yes
20	3-NO ₂	CH ₃	4-CH ₃ OC ₆ H ₄	341.40	3.16	4	0	4	70.65	High	Yes	Yes
21	3-NO ₂	CH ₃	4-Cl-C ₆ H ₄	315.75	2.84	3	0	3	61.42	High	Yes	Yes
22	4-CH ₃	CH ₃	C ₆ H ₅	250.34	3.43	1	0	2	15.60	High	Yes	Yes
23	4-CH ₃	CH ₃	4-CH ₃ OC ₆ H ₄	280.36	3.42	2	0	3	24.83	High	Yes	Yes
24	4-CH ₃	CH ₃	4-Cl-C ₆ H ₄	284.78	3.98	1	0	2	15.60	High	Yes	Yes
25	4-OCH ₃	CH ₃	C ₆ H ₅	266.34	3.12	2	0	3	24.83	High	Yes	Yes
26	4-OCH ₃	CH ₃	4-CH ₃ OC ₆ H ₄	296.36	3.08	3	0	4	34.06	High	Yes	Yes
27	4-OCH ₃	CH ₃	4-Cl-C ₆ H ₄	300.78	3.64	2	0	3	24.83	High	Yes	Yes
28	4-Br	CH ₃	C ₆ H ₅	315.21	3.74	1	0	2	15.60	High	Yes	Yes
29	4-Br	CH ₃	4-CH ₃ OC ₆ H ₄	345.23	3.71	2	0	3	24.83	High	Yes	Yes
30	4-Br	CH ₃	4-Cl-C ₆ H ₄	349.65	4.27	1	0	2	15.60	High	Yes	Yes

31	H	isopropyl	C ₆ H ₅	264.36	3.74	1	0	3	15.60	High	Yes	Yes
32	H	isopropyl	4-CH ₃ OC ₆ H ₄	294.39	3.70	2	0	4	24.83	High	Yes	Yes
33	H	isopropyl	4-Cl-C ₆ H ₄	298.81	4.27	1	0	3	15.60	High	Yes	Yes
34	3-NO ₂	isopropyl	C ₆ H ₅	309.36	2.92	3	0	4	61.42	High	Yes	Yes
35	3-NO ₂	isopropyl	4-CH ₃ OC ₆ H ₄	339.39	2.95	4	0	5	70.65	High	Yes	Yes
36	3-NO ₂	isopropyl	4-Cl-C ₆ H ₄	343.81	3.48	0	3	4	61.42	High	Yes	Yes
37	4-CH ₃	isopropyl	C ₆ H ₅	278.39	4.06	1	0	3	15.60	High	Yes	Yes
38	4-CH ₃	isopropyl	4-CH ₃ OC ₆ H ₄	308.42	4.05	2	0	4	24.83	High	Yes	Yes
39	4-CH ₃	isopropyl	4-Cl-C ₆ H ₄	312.84	4.60	1	0	3	15.60	High	Yes	Yes
40	4-OCH ₃	isopropyl	C ₆ H ₅	294.39	3.72	2	0	4	24.83	High	Yes	Yes
41	4-OCH ₃	isopropyl	4-CH ₃ OC ₆ H ₄	324.42	3.69	3	0	5	34.06	High	Yes	Yes
42	4-OCH ₃	isopropyl	4-Cl-C ₆ H ₄	328.84	4.25	2	0	4	24.83	High	Yes	Yes
43	4-Br	isopropyl	C ₆ H ₅	343.26	4.34	1	0	3	15.60	High	Yes	Yes
44	4-Br	isopropyl	4-CH ₃ OC ₆ H ₄	373.29	4.33	2	0	4	24.83	High	Yes	Yes
45	4-Br	isopropyl	4-Cl-C ₆ H ₄	377.71	4.88	1	0	3	15.60	High	Yes	Yes

Table 1. ADME properties of the designed pyrazole derivatives predicted using the SwissADME web-based tool HBAs: No. of H-bond acceptors; HBDs: No. of H-bond donors; NRBs: No. of rotatable bonds; TPSA: Topological surface area; GI ab.: Gastro-intestinal absorption; BBB permeant: Blood-brain barrier permeation.

Molecular Docking:

Inflammation is a critical pathological process underlying various chronic diseases, and the identification of safe and effective anti-inflammatory agents remains a major challenge in drug development [47-48]. In this context, *in-silico* virtual screening has emerged as a powerful and cost-effective strategy to identify potential therapeutic candidates by rapidly predicting molecular interactions between target proteins and ligand molecules [49-53]. To evaluate the affinity and binding interactions of the designed pyrazole derivatives within the active site of human PDE7 protein, *in-silico* molecular docking studies were performed using AutoDock Vina. The accuracy of the docking methodology was confirmed by the re-docked ligand, which yielded a binding pose like that of the co-crystallized PDE7 inhibitor with a ΔG of -8.9 kcal/mol (**Fig 1**). The designed pyrazole derivatives were docked into the active site of PDE7. The docking score as well as residues involved in binding interactions of the designed pyrazole derivatives with PDE7 are presented in **Table 2**.

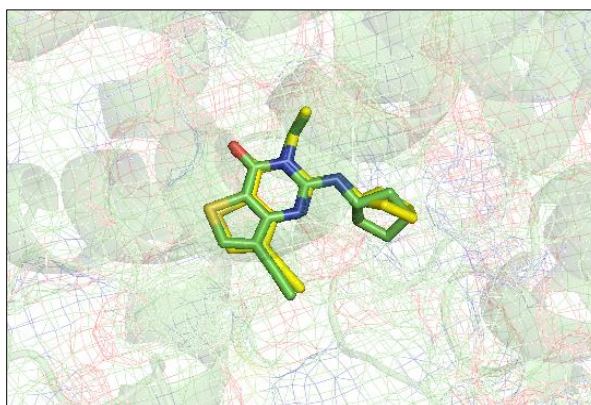


Fig 1. Validation of the docking protocol. The docking protocol was validated via redocking the co-crystallized ligand of PDE7. The re-docked ligand (yellow) produced a pose similar to that of the co-crystallized ligand (green).

Ligand	ΔG	Residues involved in hydrogen bonding (bond distance)	Hydrophobic interactions (residues involved)
1	-8.3	-	Pi-Pi (Phe384 & Phe416), Pi-Charge (Asp362), and Pi-Alkyl (Ile324 & Val380)
2	-8.6	Tyr211 (3.13Å)	Pi-Pi (His212 & Phe416), Carbon Hydrogen Bond (Asp362), and Pi-Sigma (Val380)
3	-7.0	-	Pi-Pi (His212, Phe384, & Phe416), and Pi-Alkyl (Val380, Leu401, & Ile412)
4	-8.8	Gln413 (3.17 Å)	Pi-Pi (Tyr211, & Phe416), and Pi-Sigma (Ile323, & Val380)
5	-8.5	Asn365 (2.86Å)	Pi-Pi (Phe416), and Pi-Sigma (Ile323, & Val380)
6	-9.2	Tyr211 (3.20 Å), Asp362 (3.26 Å), and Gln413 (3.09 Å)	Pi-Pi (His212, & Phe416), Pi-Donor Hydrogen Bond (Phe416), Alkyl (Leu281), Pi-Alkyl (His256), and Pi-Sigma (Val380)
7	-7.4	-	Pi-Pi (Phe384, & Phe416), Pi-Alkyl (Ile323, Val380, Leu401, & Ile412), and Pi-Anion (Asp362)
8	-8.5	Gln413 (2.81 Å)	Pi-Pi (Tyr211, & Phe416), Pi-Sigma (Ile323, & Val380), and Pi-Alkyl (Phe384, & Ile412)
9	-7.4	-	Pi-Pi (His212, Phe384, & Phe416), Pi-Alkyl (His256, Leu281, Val380, Leu401, & Ile412)
10	-8.4	Gln413 (2.83 Å)	Pi-Pi (Tyr211, & Phe416), Carbon Hydrogen Bond (Asn365), and Pi-Sigma (Val380)
11	-8.5	Gln 413 (2.81 Å)	Pi-Pi (Phe416), Pi-Alkyl (His 212, & His256), Carbon Hydrogen Bond (Asn365), and Pi-Sigma (Val380)
12	-9.1	Asp362 (3.21 Å), and Gln413 (2.89 Å)	Pi-Pi (Tyr211, & Phe416), Carbon Hydrogen Bond (Asn365), Pi-Alkyl (Leu 281, & Val380), Pi-Alkyl (Val380), and Pi-Sigma (Ile323)
13	-8.3	Asp362 (3.08Å)	Pi-Pi (Phe416), Pi-Alkyl (Val380), and Pi-Sigma (Ile323)
14	-8.8	Gln 413 (3.23 Å), and Asp362 (3.48 Å)	Pi-Pi (His212, Phe384, & Phe416), and Pi-Alkyl (Leu 281, His256, Val380, & Ile412),

15	-8.4	-	Pi-Pi (Phe384, & Phe416), and Pi-Alkyl (His256, Leu 281, His285, Val380, & Ile412)
16	-7.9	-	Pi-Pi (His212, & Phe416), Pi-Sigma (Val380), and Pi-Alkyl (His212)
17	-8.3	Asn365 (3.50 Å), and Gln413 (2.94 Å)	Pi-Pi (Tyr211, His212, & Phe416), Carbon Hydrogen Bonds (His212, & Asp362), and Pi-Alkyl (Val380)
18	-8.7	-	Pi-Pi (Phe416), Pi-Alkyl (Val380), Carbon Hydrogen Bonds (His212, & Asp362), and Pi-Sigma (Ile323)
19	-8.8	-	Pi-Pi (Phe416), and Pi-Sigma (Ile323, & Val380)
20	-9.4	Gln413 (2.97 Å)	Pi-Pi (Tyr211, & Phe416), Carbon Hydrogen Bonds (His212, & Asp362), Alkyl (Leu281, & Ile323), Pi-Sigma (Ile323, & Val380), and Pi-Alkyl (Phe416)
21	-9.6	Gln413 (2.95 Å)	Pi-Pi (Tyr211, & Phe416), Carbon Hydrogen Bonds (His212, & Asp362), Alkyl (Ile363), Pi-Sigma (Ile323, & Val380), and Pi-Alkyl (Phe416)
22	-8.6	Tyr211 (3.80 Å), and Asp362 (3.39 Å)	Pi-Pi (Phe384, & Phe416), and Pi-Alkyl (Val380, & Ile412)
23	-8.4	Asp362 (3.21 Å)	Pi-Pi (Tyr211, & Phe416), Pi-Alkyl (His212, Leu281, Phe384, & Ile412), and Pi-Sigma (Val380)
24	-8.9	His212 (3.64 Å), and Asp362 (3.59 Å)	Pi-Pi (Phe384, & Phe416), Pi-Sigma (Ile323), Pi-Alkyl (Leu281, Val380, & Ile412)
25	-8.5	Gln413 (2.82 Å)	Pi-Pi (Tyr211, & Phe416), Carbon Hydrogen Bond (Asn365), and Pi-Sigma (Val380)
26	-8.2	Gln413 (2.97 Å)	Pi-Pi (Tyr211, & Phe416), Pi-Sigma (Ile323, & Val380), and Pi-Alkyl (Pro262)
27	-8.5	Gln413 (2.80 Å)	Pi-Pi (Phe416), Pi-Sigma (Val380), and Pi-Alkyl (His256, & Leu281)
28	-8.4	Thr321 (3.77 Å)	Pi-Pi (Tyr211, & Phe416), Carbon Hydrogen Bond (Asp362), and Pi-Sigma (Val380)
29	-8.2	Gln413 (3.03 Å)	Pi-Pi (Phe384, & Phe416), and Pi-Alkyl (Leu281, Ile323, Val380, & Ile412)
30	-8.5	Asp362 (3.57 Å)	Pi-Pi (Tyr211, & Phe416), and Pi-Alkyl (His256, Leu281, Ile323, & Val380)
31	-8.2	-	Pi-Pi (Phe384, & Phe416), Pi-Alkyl (Ile363, & Leu401), and Pi-Sigma (Ile323)
32	-8.2	Gln413 (3.13 Å)	Pi-Pi (His212, & Phe416), and Pi-Alkyl (Ile323, Val380, & Phe384)
33	-7.0	-	Pi-Alkyl (Leu281, His256, Ile323, Ile363, Val380, Phe384, & Phe416)
34	-8.0	Tyr211 (2.87 Å)	Pi-Pi (Phe416), Pi-Alkyl (Ile323), Carbon Hydrogen Bond (Asn365), and Pi-Sigma (Val380)

35	-8.2	Tyr211 (3.01 Å), and Thr321 (3.38 Å)	Pi-Pi (Phe416), Pi-Alkyl (Ile323), Carbon Hydrogen Bond (Asp362), and Pi-Sigma (Val380)
36	-8.6	Gln261 (3.19 Å), Glu282 (3.17 Å), and Ser324 (3.04 Å)	Pi-Pi (Phe384), and Pi-Alkyl (His212, Val370, & Phe416)
37	-8.6	-	Pi-Sigma (Val380), Pi-Pi (Tyr211, & Phe416), and Pi-Alkyl (Ile323)
38	-8.6	Gln413(2.92 Å)	Pi-Pi (Phe416), Carbon Hydrogen Bond (Asn365), and Pi-Alkyl (Tyr211, His256, Leu281, His285, Val380, & Phe384)
39	-7.9	-	Pi-Pi (Tyr211, & Phe416), and Pi-Alkyl (His256, Leu281, Ile323, Pro366, & Val380)
40	-8.6	Gln413 (2.84 Å)	Pi-Sigma (Val380), Carbon Hydrogen Bond (Asn365), and Pi-Pi (Tyr211, & Phe416)
41	-7.8	Gln413 (2.78 Å)	Pi-Sigma (Val380), Pi-Pi (Phe416), Carbon Hydrogen Bond (Asn365), and Pi-Alkyl (Leu281)
42	-8.7	Gln413 (3.09 Å), and Ser377 (3.64 Å)	Pi-Sigma (Val380), Pi-Pi (Tyr211, His212, & Phe416), and Pi-Alkyl (Ile323, & Phe384)
43	-8.2	-	Pi-Sigma (Val380), Pi-Pi (Phe416), and Pi-Alkyl (Ile323)
44	-7.8	Gln413 (2.83 Å)	Pi-Pi (His212, & Phe416), Carbon Hydrogen Bond (Asn365), and Pi-Alky (His256, Leu281, His285, Pro366, Val380, & Phe384)
45	-7.9	-	Pi-Anion (Asp362), Pi-Pi (Phe384, & Phe416), Pi-Alkyl (Val380, Leu401, & Ile412), and Halogen (Glu282)

Table 2. Docking score and residues involved in binding interactions of designed molecules with the PDE7 protein (PDB ID: 4PM0).

Compounds 6, 12, 20, and 21 were selected for further detailed analysis based on their lowest binding free energy values and favorable docking interactions of the best-docked poses within the PDE7 active site among all docked molecules. An overlay of their docked poses with the co-crystallized PDE7 ligand (PDB ID: 4PM0) revealed that they exhibited similar binding patterns (**Fig 2**). **Fig 3** illustrates the hydrogen bonding and hydrophobic interactions formed between compounds 6, 12, 20, and 21 (in the docking study) and the active site residues of the human PDE7 protein.

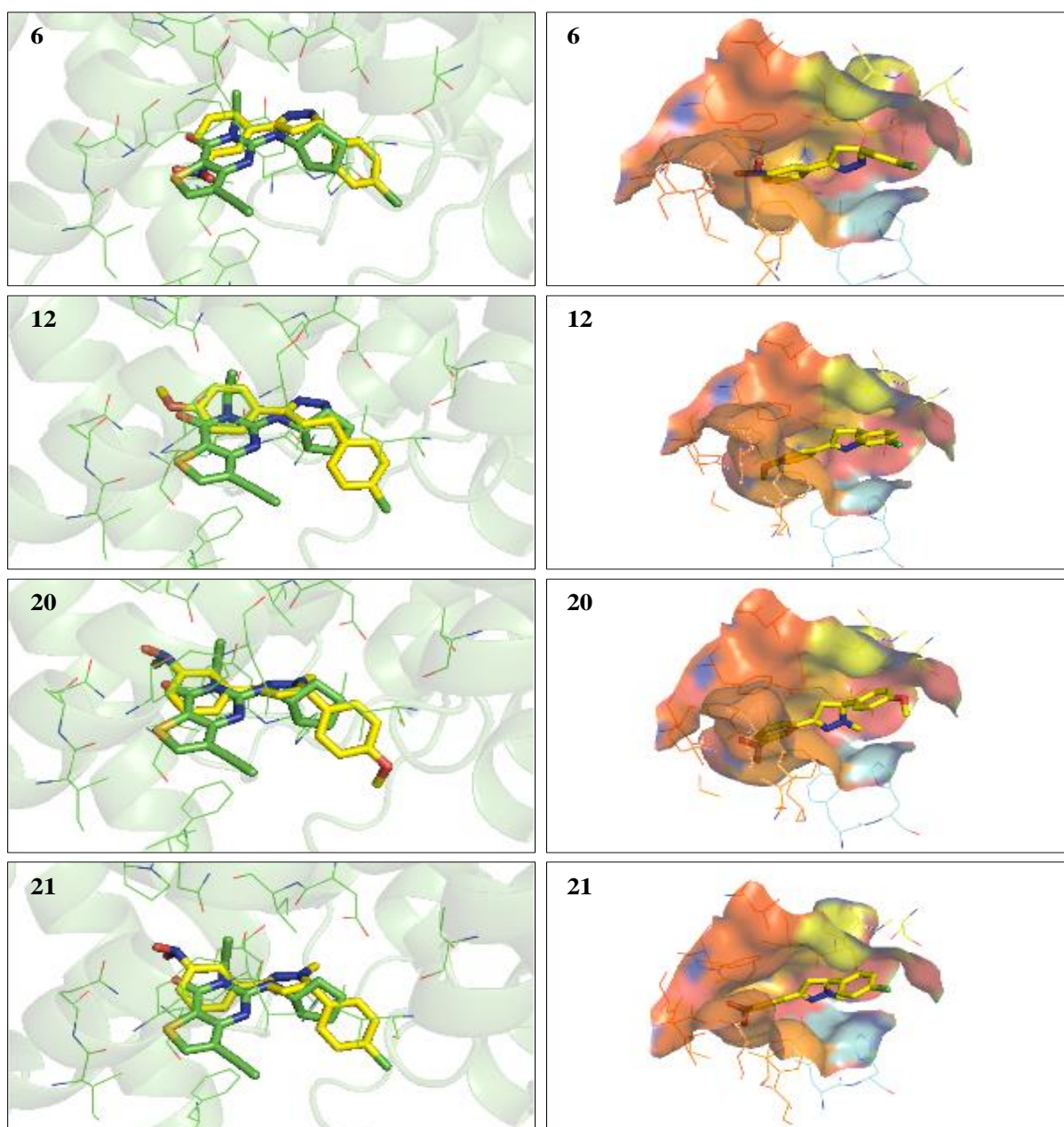


Fig 2. Left: Overlay of the docked poses of compound 6, 12, 20, and 21 (yellow) with that of the co-crystallized PDE7 ligand (green). Right: Orientation of compounds 6, 12, 20, and 21 in the active site of PDE7.

Compound 6 showed three hydrogen bonds with Tyr211 (pyrazole =N of compound 6 and -OH of Tyr211), Asp362 (pyrazole NH of compound 6 and C=O of Asp362), and Gln413 (N=O of compound 6 and NH of Gln413) with bond distances of 3.20, 3.26 and 3.09 Å, respectively, and hydrophobic interactions, i.e., Pi-Pi (His212, & Phe416), Pi-donor (Phe416), Alkyl (Leu281), Pi-Alkyl (His256), and Pi-Sigma (Val380) in the active site of PDE7. Compound 12 showed two hydrogen bonds with Asp362 (pyrazole NH of compound 12 and C=O of Asp362), and Gln413 (-O- of compound 12 and NH of Gln413) with bond distances of 3.21, and 2.89 Å, respectively) and hydrophobic interactions, i.e., Pi-Pi (Tyr211, & Phe416), Carbon Hydrogen Bond (Asn365), Pi-Alkyl (Leu 281, & Val380), Pi-Alkyl (Val380), and Pi-Sigma (Ile323) in the active site of PDE7. Compound 20 showed a hydrogen bond with Gln413 (-OH of compound 20 and C=O of Gln413) with bond distance of 2.97 Å, and hydrophobic interactions, i.e., Pi-Pi (Tyr211, & Phe416), Carbon Hydrogen Bonds (His212, & Asp362), Alkyl (Leu281, & Ile323), Pi-Sigma (Ile323, & Val380), and Pi-Alkyl (Phe416) in the active site of PDE7. Compound 21 showed a hydrogen bond with Gln413 (-OH of compound 21 and C=O of Gln413) with bond distances of 2.95 Å, and hydrophobic interactions, i.e., Pi-Pi (Tyr211, & Phe416), Carbon Hydrogen Bonds (His212, & Asp362), Alkyl (Ile363), Pi-Sigma (Ile323, & Val380), and Pi-Alkyl (Phe416) in the active site of PDE7. These *in-silico* molecular docking studies of the designed compounds with PDE7 thus helped in predicting that these compounds could act as potential inhibitors of the human PDE7 enzyme. Furthermore, the observed binding interactions can serve as a foundation for structure-activity relationship (SAR) analysis and future lead optimization efforts.

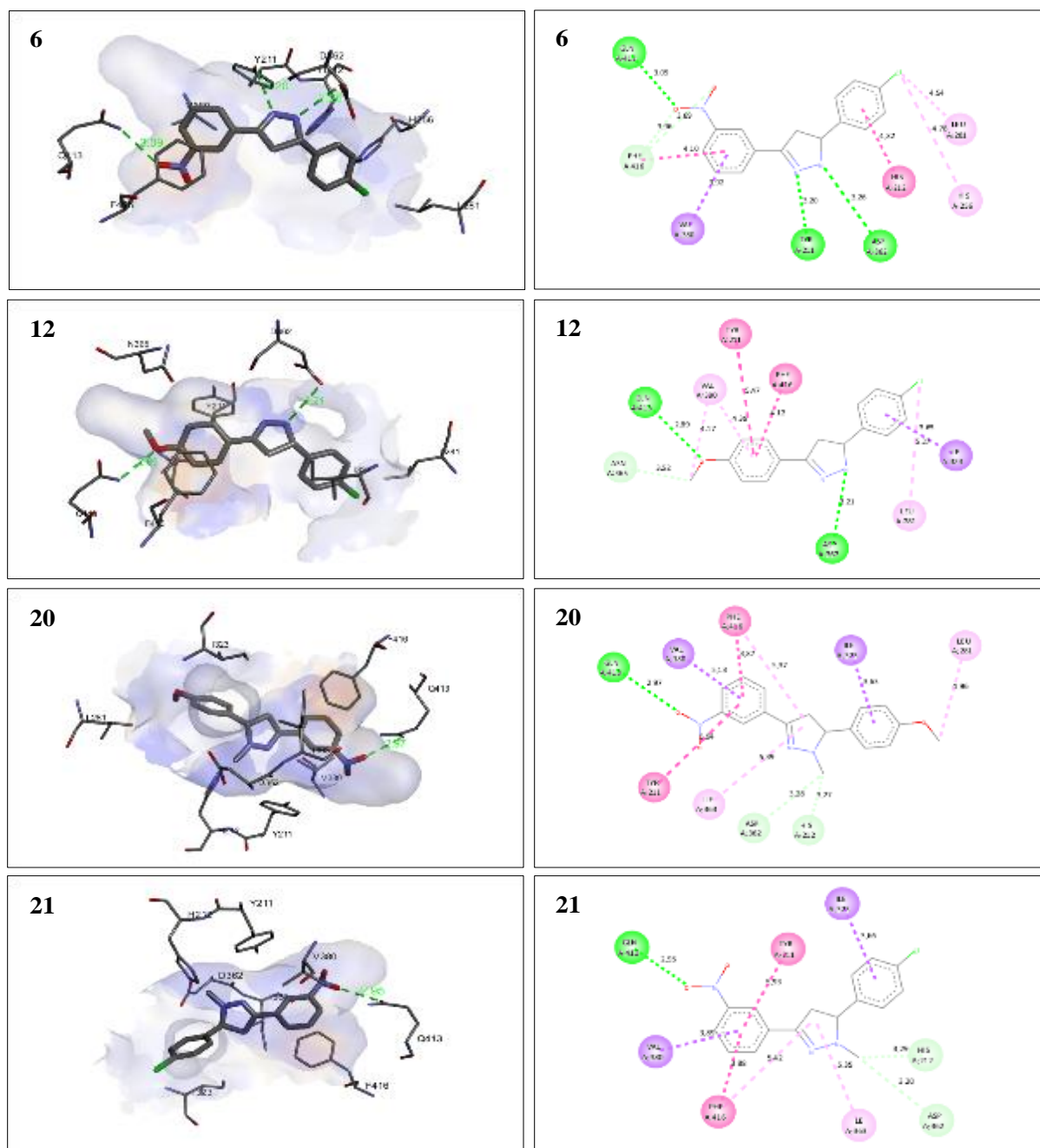


Fig 3. Interaction analysis of compounds 6, 12, 20, and 21 with PDE7. Left: 3D docked poses showing hydrogen bond interactions. Right: 2D docked poses showing hydrogen bond and hydrophobic interactions.

Prediction of Toxicity:

The potential toxicity profiles of the designed pyrazole derivatives were systematically assessed using the pkCSM online tool, which employs graph-based signatures to predict various toxicological endpoints [44-45]. The results are summarized in **Table 3**. Several compounds, such as 1, 2, 3, 4, 5, 6, 7, 9, 10, 11, 13, 15, 18, 19, 20, 21, 22, 24, 25, 27, 31, 34, 35, 36, 37, and 40 were predicted to be mutagenic. Cardiotoxicity, indicated by hERG II inhibition, was predicted for compounds 5, 9, 11, 12, 40, and 42. Hepatotoxicity was observed for compounds 5, 8, 11, 19, 20, 22, 23, 26, 29, 31, 33, 34, 35, 37, 40, and 41. Skin sensitization was predicted for compounds 1, 3, 7, 9, 13, 15, 16, 18, 22, 24, 27, 28, 30, 31, 33, 37, 39, 43, and 45. Notably, compound 5 was predicted with multiple toxicities, including mutagenicity, hepatotoxicity, and cardiotoxicity. Compound 27 was also predicted with a combination of mutagenicity, hepatotoxicity, and skin sensitization potential. The predicted maximum tolerated dose values for most compounds ranged between 0.07 to 0.64 log mg/kg/day, with lower maximum tolerated dose values suggesting a higher likelihood of toxicity at elevated doses.

Ligan	AMES toxicit	Max. tolerate	hERG I inhibitio	hERG II	Rat acute	Rat chroni	Hepato -	Skin toxicit	<i>Tetrahymen</i>	Minno w
-------	-----------------	------------------	---------------------	------------	--------------	---------------	-------------	-----------------	-------------------	------------

d	y	d dose	n	inhibiti on	tox.	c tox.	toxicity	y	a pyriformis toxicity	toxicity
1	Yes	0.230	No	No	2.532	2.003	No	Yes	1.538	0.394
2	Yes	0.301	No	No	2.353	1.335	No	No	1.766	-0.065
3	Yes	0.339	No	No	2.482	1.385	No	Yes	2.289	0.374
4	Yes	0.180	No	No	2.434	1.420	No	No	1.654	0.208
5	Yes	0.113	No	Yes	2.416	1.382	Yes	No	1.309	-0.875
6	Yes	0.190	No	NO	2.504	1.365	No	No	1.794	0.057
7	Yes	0.415	No	No	2.367	1.230	No	Yes	2.075	0.378
8	No	0.285	No	No	2.407	1.293	Yes	No	1.873	-0.214
9	Yes	0.423	No	Yes	2.497	1.137	No	Yes	2.471	0.245
10	Yes	0.375	No	No	2.308	1.130	No	No	1.788	-0.279
11	Yes	0.237	No	Yes	2.491	1.174	Yes	No	1.623	0.174
12	No	0.401	No	Yes	2,471	1.037	No	No	2.072	-0.285
13	Yes	0.411	No	No	2.471	1.146	No	Yes	2.351	0.015
14	No	0.281	No	No	2.542	1.210	No	No	2.059	-0.578
15	Yes	0.304	No	No	2.623	1.260	No	Yes	2.606	-0.265
16	No	0.385	No	No	2.014	0.826	No	Yes	2.381	0.754
17	No	0.453	No	No	2.100	0.720	No	No	2.121	-0.161
18	Yes	0.348	No	No	2.167	0.736	No	Yes	2.804	0.400
19	Yes	0.267	No	No	2.448	1.260	Yes	No	1.680	0.239
20	Yes	0.186	No	No	2.455	1.595	Yes	No	1.485	0.809
21	Yes	0.192	No	No	2.543	1.137	No	No	1.764	-0.098
22	Yes	0.350	No	No	2.010	0.785	Yes	Yes	2.547	0.478
23	No	0.465	No	No	2.070	0.679	Yes	No	2.208	-0.206
24	Yes	0.343	No	No	2.144	0.694	No	Yes	2.927	0.124
25	Yes	0.381	No	No	2.128	0.695	No	No	2.031	-0.380
26	No	0.467	No	No	2.226	1.703	Yes	No	1.704	-0.056
27	Yes	0.432	No	No	2.177	0.659	Yes	Yes	2.930	0.344
28	No	0.345	No	No	2.167	0.701	No	Yes	2.762	0.115
29	No	0.458	No	No	2.266	0.596	Yes	No	2.347	-0.570

30	No	0.339	No	No	2.291	0.611	No	Yes	3.049	-0.239
31	Yes	0.624	No	No	2.051	0.893	Yes	Yes	2.378	0.014
32	No	0.613	No	No	2.154	0.704	No	No	1.980	-1.314
33	No	0.602	No	No	2.208	0.803	Yes	Yes	2.683	-0.355
34	Yes	0.328	No	No	2.482	1.127	Yes	No	1.459	-0.487
35	Yes	0.070	No	No	2.458	1.296	Yes	No	1.142	-1.948
36	Yes	0.273	No	No	2.587	1.006	No	No	1.486	-0.839
37	Yes	0.606	No	No	2.053	0.853	Yes	Yes	2.485	-0.245
38	No	0.631	No	No	2.136	0.663	No	No	2.023	-1.339
39	No	0.602	No	No	2.191	0.763	No	Yes	2.746	-0.614
40	Yes	0.576	No	Yes	2.236	0.694	Yes	No	1.819	-1.802
41	No	0.609	No	No	2.311	1.936	Yes	No	1.600	-1.190
42	No	0.610	No	Yes	2.404	0.595	No	No	1.917	-2.079
43	No	0.607	No	No	2.263	0.745	No	Yes	2.617	-0.821
44	No	0.641	No	No	2.408	0.555	No	No	2.057	-1.915
45	No	0.604	No	No	2.385	0.655	No	Yes	2.739	-1.190

Table 3. Predicted toxicity (probability for presence or absence of toxicity) for the designed pyrazole derivatives obtained using pkCSM online tool.

AMES toxicity: Mutagenicity; Max. tolerated dose: Maximum tolerated human dose (log mg/kg/day); hERG I & II inhibition: Cardio-toxicity; Rat acute tox.: Oral rat acute toxicity (LD₅₀) (mol/kg); Rat chronic tox.: Oral rat chronic toxicity (LOAEL) (log mg/kg_bw/day); Skin toxicity: Skin sensitization.

CONCLUSION

In conclusion, it was found that there are many new pyrazole analogues to potentially be used as PDE7 inhibitors due to their high binding affinities, high drug-like properties, and expected oral bioavailability. Compounds 6, 12, 20, and 21, exhibited significant interactions with the catalytic domain of PDE7, suggesting their potential efficacy as anti-inflammatory agents. However, toxicity predictions indicated that some compounds may present risks of mutagenicity, hepatotoxicity, or skin sensitization, highlighting the need for careful optimization. While the current *in-silico* findings is encouraging, further experimental validation through *in vitro* enzymatic assays and *in-vivo* studies is essential to confirm their therapeutic potential and safety profiles. Future efforts should focus on refining this scaffold to enhance efficacy and minimize toxicity, advancing the development of safe and effective PDE7-targeted anti-inflammatory therapies.

CONFLICT OF INTEREST

The authors declare no conflict of interest.

ACKNOWLEDGMENTS

The authors extend their gratitude to the Career Point University, Hamirpur, Himachal Pradesh, India for their generous support.

REFERENCES

1. Nathan C. Nonresolving inflammation redux. *Immunity.* 2022; 55(4): 592-605. doi: 10.1016/j.immuni.2022.03.016.
2. Hirano T. IL-6 in inflammation, autoimmunity and cancer. *International Immunology.* 2021; 33(3): 127-148. doi: 10.1093/intimm/dxaa078.
3. Singh A, Schurman SH, Bektas A, Kaileh M, Roy R, Wilson DM, Ferrucci L. Aging and inflammation. *Cold Spring Harbor Perspectives in Medicine.* 2024; 14(6): a041197. doi: 10.1101/cshperspect.a041197.
4. Gusev E, Zhuravleva Y. Inflammation: A new look at an old problem. *International Journal of Molecular Sciences.* 2022; 23(9): 4596. doi: 10.3390/ijms23094596.
5. Oronsky B, Caroen S, Reid T. What exactly is

- inflammation (and what is it not?). *International Journal of Molecular Sciences.* 2022; 23(23): 14905. doi: 10.3390/ijms232314905.
6. Pezone A, Olivieri F, Napoli MV, Procopio A, Avvedimento EV, Gabrielli A. Inflammation and DNA damage: cause, effect or both. *Nature Reviews Rheumatology.* 2023; 19(4): 200-211. doi: 10.1038/s41584-022-00905-1.
7. Soysal P, Arik F, Smith L, Jackson SE, Isik AT. Inflammation, frailty and cardiovascular disease. *Advances in Experimental Medicine and Biology.* 2020; 1216: 55-64. doi: 10.1007/978-3-030-33330-0_7.
8. Hannood S, Nasuruddin DN. Acute inflammatory response. In: StatPearls [Internet]. StatPearls Publishing 2024.
9. Akiyama Y, Yao JR, Kreder KJ, O'Donnell MA, Lutgendorf SK, Lyu D, Luo Y. Autoimmunity to urothelial antigen causes bladder inflammation, pelvic pain, and voiding dysfunction: a novel animal model for Hunner-type interstitial cystitis. *American Journal of Physiology Renal Physiology.* 2021; 320(2): F174-F182. doi: 10.1152/ajprenal.00290.2020.
10. Xia Y, Xia C, Wu L, Li Z, Li H, Zhang J. Systemic immune inflammation index (SII), system inflammation response index (SIRI) and risk of all-cause mortality and cardiovascular mortality: a 20-year follow-up cohort study of 42,875 US adults. *Journal of Clinical Medicine.* 2023; 12(3): 1128. doi: 10.3390/jcm12031128.
11. Ishijima T, Nakajima K. Inflammatory cytokines TNF α , IL-1 β , and IL-6 are induced in endotoxin-stimulated microglia through different signaling cascades. *Science Progress.* 2021; 104(4): 00368504211054985. doi: 10.1177/00368504211054985.
12. Dey R, Dey S, Samadder A, Saxena AK, Nandi S. Natural inhibitors against potential targets of cyclooxygenase, lipooxygenase and leukotrienes. *Combinatorial Chemistry & High Throughput Screening.* 2022; 25(14): 2341-2357. doi: 10.2174/1386207325666210917111847.
13. Sarapultsev A, Gusev E, Komelkova M, Utepova I, Luo S, Hu D. JAK-STAT signaling in inflammation and stress-related diseases: implications for therapeutic interventions. *Molecular Biomedicine.* 2023; 4(1): 40. doi: 10.1186/s43556-023-00151-1.
14. Liu J, Han X, Zhang T, Tian K, Li Z, Luo F. Reactive oxygen species (ROS) scavenging biomaterials for anti-inflammatory diseases: from mechanism to therapy. *Journal of Hematology & Oncology.* 2023; 16(1): 116. doi: 10.1186/s13045-023-01512-7.
15. Jaén RI, Sánchez-García S, Fernández-Velasco M, Boscá L, Prieto P. Resolution-based therapies: the potential of lipoxins to treat human diseases. *Frontiers in Immunology.* 2021; 12: 658840. doi: 10.3389/fimmu.2021.658840.
16. Wirth T, Lafforgue P, Pham T. NSAID: Current limits to prescription. *Joint Bone Spine* 2024; 91(4): 105685. doi: 10.1016/j.jbspin.2023.105685.
17. Livshits G, Kalinkovich A. Targeting chronic inflammation as a potential adjuvant therapy for osteoporosis. *Life Sciences.* 2022; 306: 120847. doi: 10.1016/j.lfs.2022.120847.
18. Rah B, Rather RA, Bhat GR, Baba AB, Mushtaq I, Farooq M, Afroze D. JAK/STAT signaling: molecular targets, therapeutic opportunities, and limitations of targeted inhibitions in solid malignancies. *Front Pharmacol* 2022; 13: 821344.
19. Zorn A, Baillie G. Phosphodiesterase 7 as a therapeutic target—Where are we now? *Cell Signal* 2023; 108: 110689.
20. Prabowo B, Mardining Raras TY, Lusida MLI, Barlianto W, Sujuti H, Mustamsir E, Drajat RS, Prawiro SR. Roles of anti-inflammatory active ingredients of *Saussurea costus*: *in-silico* approach as adjuvant therapy in COVID-19 cases. *Res J Pharm Technol* 2023; 16(6): 2649-2654.
21. Balasundaram A, David DC. Evaluating phosphodiesterase 7B inhibition by vasicine using nuclear magnetic resonance spectroscopy. *Res J Pharm Technol* 2023; 16(1): 103-106.
22. Szczypka M. Role of phosphodiesterase 7 (PDE7) in T cell activity. Effects of selective PDE7 inhibitors and dual PDE4/7 inhibitors on T cell functions. *Int J Mol Sci* 2020; 21(17): 6118.
23. Epstein PM, Basole C, Brocke S. The role of PDE8 in T cell recruitment and function in inflammation. *Front Cell Dev Biol* 2021; 9: 636778.
24. Li G, Cheng Y, Han C, Song C, Huang N, Du Y. Pyrazole-containing pharmaceuticals: target, pharmacological activity, and their SAR studies. *RSC Med Chem* 2022; 13(11): 1300-1321.
25. Selvam TP, Saravanan G, Prakash CR, Kumar PD. Microwave-assisted synthesis, characterization and biological activity of novel pyrazole derivatives. *Asian Journal of Pharmaceutical Research.* 2011; 1(4): 126-129.
26. Balaji PN, Prathusha K, Chandu TJ, Sreevani MS, Rani PJ, Harini P. Synthesis, characterization and antimicrobial activity of some synthesized isoxazole and pyrazole derivatives. *Asian Journal of Research in Chemistry.* 2011; 4(2): 301-303.
27. Patil P, Sridhar S, Anusha V, Vishwanatham Y, Swamy K, Suman D. Synthesis, characterisation and evaluation of anti-inflammatory activity of some new aryl pyrazole derivatives. *Asian Journal of Research in Chemistry,* 2014; 7(3): 269-274.
28. Sudeep S, Tathagata D, Somila K, Jyothi Y. Microwave assisted synthesis of fluoro-pyrazole derivatives for antiinflammatory activity. *Research Journal of Pharmacy and Technology.* 2011; 4(3): 413-419.
29. Zhou Y, Li J, Yuan H, Su R, Huang Y, Huang Y, Huang L. Design, synthesis, and evaluation of dihydropyranopyrazole derivatives as novel PDE2 inhibitors for the treatment of Alzheimer's disease. *Molecules.* 2021; 26(10): 3034.
30. Abdel-Halim M, Tinsley H, Keeton AB, Weam M,

- Atta NH, Hammam MA, Abadi AH. Discovery of trisubstituted pyrazolines as a novel scaffold for the development of selective phosphodiesterase 5 inhibitors. *Bioorganic Chemistry.* 2020; 104: 104322. doi: 10.1016/j.bioorg.2020.104322.
31. Singh K, Kumari S, Gupta YK. Synthesis and antimicrobial activity of new pyrazoles and chalcones derived from cyclic imides. *Research Journal of Pharmacy and Technology.* 2017; 10(12): 4483-4488.
32. Kumari MA, Venkatarao C. A review on recent trends in the bioactive studies of pyrazole derivatives. *Asian Journal of Research in Chemistry.* 2020; 13(5): 383-394.
33. Shinde NG, Pimpodkar NV. Pharmacological significance of pyrazole and its derivatives. *Research Journal of Pharmaceutical Dosage Forms and Technology.* 2015; 7(1): 74-81.
34. Rocha S, Silva J, Silva VLM, Silva AMS, Corvo ML, Freitas M, Fernandes E. Pyrazoles have a multifaceted anti-inflammatory effect targeting prostaglandin E2, cyclooxygenases and leukocytes' oxidative burst. *International Journal of Biochemistry & Cell Biology.* 2024; 172: 106599. doi: 10.1016/j.biocel.2024.106599.
35. Alam MJ, Alam O, Naim MJ, Nawaz F, Manaithiya A, Imran M, Thabet HK, Alshehri S, Ghoneim MM, Alam P, Shakeel F. Recent advancement in drug design and discovery of pyrazole biomolecules as cancer and inflammation therapeutics. *Molecules.* 2022; 27(24): 8708.
36. Shaker AMM, Shahin MI, AboulMagd AM, Abdel Aleem SA, Abdel-Rahman HM, Abou El Ella DA. Novel 1,3-diaryl pyrazole derivatives bearing methylsulfonyl moiety: Design, synthesis, molecular docking and dynamics, with dual activities as anti-inflammatory and anticancer agents through selectively targeting COX-2. *Bioorganic Chemistry.* 2022; 129: 106143. doi: 10.1016/j.bioorg.2022.106143.
37. Abd-Rabo ZS, George RF, Zaafar DK, Gawish AY, Serry AM. Design, synthesis, and biological evaluation of some new 2-phenyl-3,6-pyridazinedione derivatives as PDE-5 inhibitors. *Bioorganic Chemistry.* 2024; 145: 107213. doi: 10.1016/j.bioorg.2024.107213.
38. Daina A, Michielin O, Zoete V. SwissADME: a free web tool to evaluate pharmacokinetics, drug-likeness and medicinal chemistry friendliness of small molecules. *Scientific Reports.* 2017; 7: 42717. doi: 10.1038/srep42717.
39. Suganya J, Manoharan S, Radha M, Singh N, Francis A. Identification and analysis of natural compounds as fungal inhibitors from *Ocimum sanctum* using *in-silico* virtual screening and molecular docking. *Research Journal of Pharmacy and Technology.* 2017; 10(10): 3369-3374.
40. Lipinski CA, Lombardo F, Dominy BW, Feeney PJ. Experimental and computational approaches to estimate solubility and permeability in drug discovery and development settings. *Advanced Drug Delivery Reviews.* 2001; 46(1-3): 3-26. doi: 10.1016/s0169-409x(00)00129-0.
41. Morris GM, Huey R, Lindstrom W, Sanner MF, Belew RK, Goodsell DS, Olson AJ. AutoDock4 and AutoDockTools4: Automated docking with selective receptor flexibility. *Journal of Computational Chemistry.* 2009; 30(16): 2785-2791. doi: 10.1002/jcc.21256.
42. Trott O, Olson AJ. AutoDock Vina: improving the speed and accuracy of docking with a new scoring function, efficient optimization, and multithreading. *Journal of Computational Chemistry.* 2010; 31(2): 455-461. doi: 10.1002/jcc.21334.
43. Rathee D, Lather V, Grewal AS, Dureja H. Enzymatic inhibitory activity of iridoid glycosides from *Picrorhiza kurroa* against matrix metalloproteinases: Correlating in vitro targeted screening and docking. *Computational Biology and Chemistry.* 2019; 78: 28-36. doi: 10.1016/j.compbiolchem.2018.10.017.
44. Pires DEV, Kaminskas LM, Ascher DB. Prediction and optimization of pharmacokinetic and toxicity properties of the ligand. *Methods in Molecular Biology.* 2018; 1762: 271-284. doi: 10.1007/978-1-4939-7756-7_14.
45. Pires DE, Blundell TL, Ascher DB. pkCSM: Predicting small-molecule pharmacokinetic and toxicity properties using graph-based signatures. *Journal of Medicinal Chemistry.* 2015; 58(9): 4066-4072. doi: 10.1021/acs.jmedchem.5b00104.
46. Veber DF, Johnson SR, Cheng HY, Smith BR, Ward KW, Kopple KD. Molecular properties that influence the oral bioavailability of drug candidates. *Journal of Medicinal Chemistry.* 2002; 45(12): 2615-2623. doi: 10.1021/jm020017n.
47. Chen L, Deng H, Cui H, Fang J, Zuo Z, Deng J, Li Y, Wang X, Zhao L. Inflammatory responses and inflammation-associated diseases in organs. *Oncotarget.* 2017; 9(6): 7204-7218. doi: 10.18632/oncotarget.23208.
48. Raizada S, Obukhov AG, Bharti S, Wadhonkar K, Baig MS. Pharmacological targeting of adaptor proteins in chronic inflammation. *Inflammation Research.* 2024; 73(10): 1645-1656. doi: 10.1007/s00011-024-01921-5.
49. Alonso H, Bliznyuk AA, Gready JE. Combining docking and molecular dynamic simulations in drug design. *Medicinal Research Reviews.* 2006; 26(5): 531-568. doi: 10.1002/med.20067.
50. Sadybekov AV, Katritch V. Computational approaches streamlining drug discovery. *Nature.* 2023; 616(7958): 673-685. doi: 10.1038/s41586-023-05905-z.
51. Patil VS, Patil PA. Molecular Docking: A useful approach of drug discovery on the basis of their structure. *Asian Journal of Pharmaceutical Research.* 2023; 13(3): 191-195.
52. Ramjith US, Shahin M. Molecular Docking Study of Novel Imidazo[2,1-b]-1,3,4 thiadiazole derivatives.

Research Journal of Pharmacy and Technology.
2013; 6(6): 688-694.

53. Napoleon AA, Sharma V. Molecular docking and in-vitro anti-inflammatory evaluation of novel isochromen-1-one analogues from etodolac. Research Journal of Pharmacy and Technology. 2017; 10(8): 2446-2450.